NACA RM L55E24

NACA

RESEARCH MEMORANDUM

DRAG INVESTIGATION OF A SWEPT-WING FIGHTER-AIRPLANE MODEL INCORPORATING TWO DRAG-RISE-REDUCING FUSELAGE REVISIONS

By Charles F. Whitcomb and Edwin E. Lee, Jr.

Langley Aeronautical Laboratory
Langley Field, Va.

NATIONAL ADVISORY COMMITTEE
FOR AERONAUTICS

WASHINGTON

July 19, 1955
Declassified December 21, 1959

NATIONAL ADVISORY COMMITTEE FOR AERONAUTICS

RESEARCH MEMORANDUM

DRAG INVESTIGATION OF A SWEPT-WING FIGHTER-AIRPLANE MODEL INCORPORATING TWO DRAG-RISE-REDUCING FUSELAGE REVISIONS

By Charles F. Whitcomb and Edwin E. Lee, Jr.

SUMMARY

Several configurations of a 45° swept-wing fighter-airplane force model were investigated in the Langley 16-foot transonic tunnel at low lifts between Mach numbers of 0.80 and 1.10 to determine the effects of modified applications of the transonic and supersonic area rules on the transonic drag-rise characteristics of the model. Fuselage indentations were limited so as to compensate for approximately 50 percent of the maximum cross-sectional area of the wing, and cusps were eliminated from the remaining area-development contour by adding fuselage volume, in order to maintain practical airplane fuselage contours and capacities. In addition to data showing the effects of fuselage revision on drag, the lift and pitching-moment characteristics of all configurations tested are presented.

Revisions to the longitudinal area development of the model to compensate for only a portion of the wing cross-sectional areas, and removal of cusps in the area-development contours based on transonic-area-rule considerations, resulted in a reduction in the transonic minimum-drag-coefficient rise of the order of 57 percent at a Mach number of 1.0 and 31 percent at a Mach number of 1.07.

At a Mach number of 1.0, similar partial fuselage revisions based on the supersonic-area-rule concepts for a Mach number of 1.2 produced drag-rise reductions essentially the same as those obtained from the transonic-area-rule model. Theoretical zero-lift drag-rise estimates for all three configurations agreed with experimental values well within the accuracy limitations of the method.

In general, applications of the transonic and supersonic area rules produced a slight increase in lift-curve slope and more positive pitching-moment coefficients throughout the Mach number range, and also slightly reduced the stability between lift coefficients of -0.15 and 0.15 at Mach numbers from 0.93 to 1.00.

INTRODUCTION

Fuselage indentations designed to modify longitudinal cross-sectional-area distributions of models in conformance with the transonic area rule of reference 1 have proven effective in reducing the zero-lift drag rise. The adaptation of such drag-reducing indentations to practical military aircraft configurations generally involves a considerable compromise with ideal considerations because of space limitations and aircraft requirements other than high cruising Mach numbers. Some recent work has been done in an attempt to achieve a more practical means of applying the area rule. Reference 2 investigated a swept wing-body research model which incorporated asymmetrical body indentations that compensated for only 50 percent of the normal cross-sectional areas of the wing. In that case the drag-rise reduction was somewhat greater than 50 percent of that realized by compensating for the complete cross-sectional area of the wing. Also, a second procedure for practical application of the area rule was devised theoretically in reference 3 and verified experimentally in references 4 and 5. That is, adding fuselage volume to remove reversals in longitudinal area-development contours will reduce the transonic drag rise of a model.

In addition to the transonic area rule, a more recent supersonic area rule has been developed (refs. 6 and 7) which associates the supersonic wave drag, or pressure drag, of the configuration with its longitudinal area distribution. The body modifications for drag reduction may be designed for optimum results at one specific supersonic Mach number with this method.

In the present investigation several configurations of a swept-wing fighter-airplane model were tested to determine the effects of incorporating modified versions of the transonic and supersonic area rules on the transonic drag-rise characteristics of the model over the low lift range. Approximately 50 percent of the maximum cross-sectional areas of the wing as determined for both area rules (supersonic area at a Mach number of 1.2) was compensated for by fuselage indentation, and the remaining area-development-contour cusps were eliminated by adding fuselage volume. Theoretical estimates of the zero-lift drag rise of the basic and two revised configurations have been determined for a low supersonic Mach number by the linearized-flow method presented in reference 3, and are included for comparison with the experimental values. Results obtained from tests of the basic fuselage and the fuselage with empennage are also included.

SYMBOLS

A	cross-sectional area
$\bar{c}$	mean aerodynamic chord
C_L	lift coefficient, $\frac{\text{Lift}}{qS}$
C_D	drag coefficient, $\frac{\text{Drag}}{qS}$
$C_{D_{min}}$	minimum drag coefficient, $\frac{\text{Minimum drag}}{qS}$
$\Delta C_{D_{min}}$	minimum-drag-coefficient rise, $\left(C_{D_{min}}\right)_{M>0.85} - \left(C_{D_{min}}\right)_{M=0.85}$
C_m	pitching-moment coefficient, $\frac{\text{Pitching moment about } 0.35\bar{c}}{qS\bar{c}}$
$\frac{L}{D}$	lift-drag ratio
l	fuselage or body length
M	Mach number
P_B	base pressure coefficient, $\frac{p_B - p_o}{q}$
p_B	base static pressure
p_o	free-stream static pressure
q	free-stream dynamic pressure
R	Reynolds number
S	wing area
x	local fuselage or body station
α	angle of attack, deg

θ roll angle of Mach planes relative to model axis system, deg

Subscripts:

av average

min minimum

max maximum

APPARATUS AND METHODS

Tunnel and Models

The investigation was conducted in the Langley 16-foot transonic tunnel, for which the air-flow and power characteristics are presented in reference 8. The basic model used was a sting-mounted fighter-airplane configuration. The wing had a 45° sweepback angle along the 0.25-chord line, a taper ratio of 0.3, an aspect ratio of 3.56, and NACA $64_{(06)}$A007 airfoil sections in planes parallel to the plane of symmetry. The horizontal and vertical tails had essentially the same geometry as the wing. Figure 1 presents a three-view sketch of the basic model and its fuselage revisions. Photographs of the basic model and the model with the transonic-area-rule modifications are presented as figure 2. A table of the model dimensional details is given in reference 9. The basic model was of all-metal construction with the exception of the wooden canopy, tail fillet, faired nose section, and wing leading-edge segments to the 0.20-chord line. Each of the two revised-area-distribution fuselages was of all-wood construction. All tests were made with the fuselage and canopy as an integral unit and subsequent reference to the fuselage should be understood to include the canopy. For the tests of the two incomplete configurations, flush wooden fairings were used to complete the model contours. A horizontal-tail setting of 0° was used for all tests of configurations with empennage.

Design of Fuselage Revisions

Transonic-area-rule configuration.- The transonic area rule was applied to the fuselage as follows: The normal cross-sectional-area distributions of the several components (wing, fuselage, canopy, and empennage) of the basic configuration were obtained and totaled to determine the equivalent-body area development (see fig. 3(a)). At the longitudinal station of maximum cross-sectional area, 50 percent of the

local cross-sectional area of the wing was subtracted from the cross-sectional area of the equivalent body. Curves were then drawn fore and aft of this point, tangent to the total-cross-sectional-area curves, so that the new area distribution assumed a relatively smooth contour. This contour was adapted to the model fuselage by asymmetrical cross-sectional-area indentations and/or additions. The resultant indentations were intended to be within practical full-scale airplane limitations in both size and distribution. Figure 1 presents a typical revised cross section as related to the cross section of the basic model. The revised fuselage contours in the side and plan views are also shown. The revisions increased the equivalent-body fineness ratio of the complete model from 7.0 to 7.6. The actual final revised-fuselage design introduced slight irregularities into the area distribution (see fig. 3(a) at $x/l = 0.45$). These irregularities were caused by slight errors in determining the area increments and decrements. This revised fuselage designed in accordance with transonic-area-rule considerations will be referred to as the M = 1.0 fuselage.

Supersonic-area-rule configuration.- The design of the supersonic-area-rule fuselage for a Mach number of 1.2 followed the assumptions and procedures of reference 7. That is, the model was assumed to be symmetrical about the horizontal and vertical planes, and the cross-sectional-area distributions intersected by parallel Mach planes inclined to the stream at the proper angle were obtained for the model at only three roll angles ($\theta = 0^\circ$, 45°, and 90°). The asymmetry of the vertical tail was neglected, since the oblique sectional areas of the wing only were used to approximate the supersonic equivalent-body-area development. A mean curve of the individual cross-sectional-area distributions of the wing was determined by algebraic averaging; the 45° roll-angle areas were given twice as much weight as the 0° and 90° areas, which were weighted equally. This mean weighted curve was used to define the supersonic equivalent-body area development. Figure 3(b) presents curves for the individual wing cross-sectional areas and weighted mean area superimposed on the curve for the M = 1.0 fuselage with empennage. The additional revisions made to the M = 1.0 fuselage were determined by selecting a maximum-total-area point that maintained the fineness ratio of the M = 1.0 configuration (7.6) and refairing the area contours fore and aft. The maximum indentations required, with respect to the basic fuselage, were approximately 50 percent of the maximum weighted mean area. Figure 3(c) presents the individual cross-sectional-area distributions of the wing and the weighted-mean-area curve superimposed on the M = 1.2 fuselage with empennage. Figure 3(d) presents a comparison of the area distributions of the M = 1.0 and M = 1.2 configurations as "seen" by the air stream at a Mach number of 1.0. Hereinafter, the fuselage as revised in accordance with supersonic-area-rule considerations will be referred to as the M = 1.2 fuselage.

Instrumentation

A six-component internal strain-gage balance was used to obtain the force and moment data presented. The readings of three static-pressure tubes equally spaced at annular positions about the base of the model were averaged to obtain the base pressure information.

Tests

Five model configurations were tested; the basic, M = 1.0 and M = 1.2 complete configurations, the basic fuselage with empennage, and the basic fuselage. The test angle of attack ranged from -2.3° to 5.0° and the Mach number from 0.80 to 1.10, each configuration being tested through all, or the major portion, of these ranges. The Reynolds number, based on the mean wing aerodynamic chord, ranged from 6.46×10^6 to 7.38×10^6 and is presented as a function of Mach number in figure 4.

Corrections and Accuracies

Base-pressure adjustments have been made to the model chord-force values by correcting the base pressures to free-stream static conditions. The base pressure coefficients are presented as a function of Mach number in figure 5. Other possible sting-interference effects on the forces and moments of the three complete configurations are assumed to be minimized in the presented comparisons.

Above a Mach number of approximately 1.02, tunnel boundary disturbances are known to have significantly affected the model drag data (see refs. 10 and 11). Therefore, the summary drag results have been adjusted in this Mach number range. The adjusting increments in drag coefficient were estimated from references 10 and 11 and rocket-test results presented in reference 12 for a configuration almost identical to the present basic model. The adjustments in drag coefficient varied from 0.000 to 0.003.

The absolute accuracy of the lift, drag, and pitching-moment coefficients as measured is estimated to be ± 0.01, ± 0.0015, and ± 0.002, respectively. The incremental drag coefficients are estimated to be accurate to ± 0.001. The average free-stream Mach number is accurate to ± 0.005 and the angle of attack is estimated to be accurate within $\pm 0.1^{\circ}$.

RESULTS AND DISCUSSION

The lift, drag, and pitching-moment coefficients of the wing-off configurations are presented as functions of angle of attack at the several test Mach numbers in figure 6. Figure 7 presents the lift, drag, and pitching-moment characteristics of the three complete configurations for the several test Mach numbers.

Lift and Pitching-Moment Characteristics

Lift.- The effect on the lift characteristics of applying the transonic- and supersonic-area-rule concepts to the test configuration was small. This small effect is evident in the slight increase in lift-curve slope shown in figure 7(a).

Pitching moment.- The stability characteristics shown in figure 7(c) indicate that, in general, the fuselage revisions produced more positive pitching-moment coefficients than the basic configuration throughout the test Mach number range, and also decreased the stability for lift coefficients between -0.15 and 0.15 at Mach numbers from 0.93 to 1.00.

Drag Characteristics

Variation with Mach number.- The variation of minimum drag coefficient with Mach number for all configurations is presented in figure 8. Variations at the constant lift coefficients of 0.2 and 0.35 are included for the three complete configurations only. The symbols which appear in figure 8 at Mach numbers of 1.02 and up represent the cross-faired values obtained from the drag polars, and the faired curves in that range include the previously mentioned drag adjustments to the test results. For the minimum-drag case, the slight differences in the lower subsonic drag levels of the three complete configurations may have resulted from changes in the model surface roughness (see ref. 13) and effects of the body contours on the boundary layer. As previously stated, most of the basic fuselage was fabricated of metal, whereas the two modified fuselages were all wood.

Also shown in the minimum-drag-coefficient curves is a drag-rise reversal for the complete M = 1.0 configuration between Mach numbers of 0.95 and 0.97. Although the unavailability of pressure-loads data or supplementary component-force data during these tests prevents any thorough analysis of this condition, it should be noted that similar reversals for area-rule-model tests have been noted previously. (See, for example, ref. 14.)

It may be noted from the drag coefficients presented for the complete configurations in figure 8 that the reduction in drag rise obtained for minimum-drag coefficients was maintained at lift coefficients up to 0.35.

Minimum-drag-coefficient rise.- The variation of $\Delta C_{D_{min}}$ with Mach number for all five of the test configurations is presented in figure 9. The drag coefficients at a Mach number of 0.85 have been selected as representative of the subsonic drag level of the various configurations. The partial transonic-area-rule modifications resulted in a reduction of minimum-drag-coefficient rise of 57 percent at a Mach number of 1.0 and 31 percent at a Mach number of 1.07 as compared with the values for the basic model. If the $\Delta C_{D_{min}}$ curve of the basic fuselage alone is considered to be the lowest level obtainable by ideal conformance to the area rule, then the revisions have produced 67 percent of the maximum possible reduction at a Mach number of 1.0. It is to be recalled that the M = 1.0 configuration was constructed by indenting the fuselage at the longitudinal station of maximum cross-sectional area of the equivalent body by an amount equal to only 50 percent of the wing cross-sectional area, and then adding area fore and aft of the resulting indentation to remove cusps in the contour and form a smooth equivalent body. By similar considerations, $\Delta C_{D_{min}}$ at a Mach number of 1.07 has been reduced by 54 percent. Further reduction at these Mach numbers might be achieved by conforming the equivalent-body area development to a more optimum shape, such as the theoretical Sears-Haack body.

The area-distribution comparisons of figure 3(d) indicate that the revision of the M = 1.0 model to the supersonic-area-rule configuration might have some small adverse effect on the M = 1.0 model drag-rise characteristics at a Mach number of 1.0. The results in figure 9 indicate that, at M = 1.0, the reduction in $\Delta C_{D_{min}}$ from the value for the basic model has decreased from 57 percent for the M = 1.0 model to 50 percent for the M = 1.2 model. At a Mach number of 1.07, a relatively larger decrease (from 31 to 21 percent) occurs. If some significant reduction of the supersonic drag, as theoretically predicted for axisymmetric configurations in reference 3, can be assumed to occur at the design Mach number in the case of the M = 1.2 configuration, then the small adverse drag effects encountered in the immediate transonic range are of secondary importance.

In figure 9, the minimum-drag-coefficient rise for the basic fuselage with empennage is almost identical to that for the two revised complete configurations at a Mach number of 1.0. There has been some recent interest in the possibility of obtaining a correlation between the fineness ratio of the equivalent body and its incremental drag-rise coefficient. Since the equivalent-body fineness ratio for the basic

fuselage with empennage is considerably larger than that for the complete revised configurations (see figs. 3(a) and 3(d)), such a correlation for the present tests would seem doubtful at a Mach number of 1.0.

Theoretical estimates of zero-lift drag rise.- As previously mentioned, a linearized-flow method is available for estimating the zero-lift drag-rise characteristics of a configuration (ref. 3). The zero-lift drag-coefficient rise for each of the three complete configurations has been estimated at a Mach number of 1.07. At this Mach number the limitations of the reference theory are approaching a minimum and the adjustments that must be made to the experimental drag data are approximately zero (see fig. 8). The values are presented as individual data points with symbols in figure 9, and indicate that the experimental values at a Mach number of 1.07 do not vary from the theoretical estimates for a Mach number of 1.07 by more than 15 percent for any of the three configurations. This is well within the ±20-percent accuracy estimated for this method in its original presentation. The use of experimental values of zero-lift drag-coefficient rise instead of the presented minimum-drag-coefficient rise would not change this comparison by more than 1 percent (see fig. 7(b) at $M = 1.06$ and 1.08).

Lift-drag ratios.- The variation with Mach number of the lift-drag ratios for the three complete configurations is presented at the constant lift coefficient of 0.35 in figure 10. The more desirable variation of the maximum values of the lift-drag ratios was unavailable above a Mach number of 0.95 without extrapolating the drag polars. However, the maximum values for the basic configuration up to a Mach number of 0.95 are presented in the figure as data points, to demonstrate that the ratios presented closely approach the maximum values. The high values for all three configurations in the lower subsonic Mach number range are attributed to low minimum drags. As anticipated, the two revised configurations show an appreciable increase in performance, as compared with the basic model, at Mach numbers above $M = 0.90$. No appreciable difference in the lift-drag ratios is indicated between the $M = 1.0$ and $M = 1.2$ models throughout the transonic range.

SUMMARY OF RESULTS

An investigation at transonic speeds of the effect of two types of area-rule fuselage revisions on the drag-rise characteristics of a swept-wing fighter airplane has led to the following results:

1. Asymmetrical fuselage revisions made to compensate for only a portion of the cross-sectional areas contributed by the wing and removal of cusps in the model area-development contours based on transonic-area-rule considerations led to a reduction in transonic minimum-drag-coefficient rise of the order of 57 percent at a Mach number of 1.0 and 31 percent at a Mach number of 1.07.

2. Similar asymmetric fuselage revisions based on supersonic-area-rule concepts at a Mach number of 1.2 led to a reduction in minimum-drag-coefficient rise at a Mach number of 1.0 essentially the same as that which resulted from the revisions designed specifically for a Mach number of 1.0.

3. Theoretical zero-lift drag-rise estimates calculated for the basic and two revised configurations by a linearized-flow method varied from the experimental values by a percentage somewhat less than the estimated limitations of that method.

4. In general, applications of the transonic and supersonic area rules produced a slight increase in lift-curve slope and more positive pitching-moment coefficients through the Mach number range, and also slightly reduced the stability between lift coefficients of -0.15 and 0.15 at Mach numbers from 0.93 to 1.00.

Langley Aeronautical Laboratory,
National Advisory Committee for Aeronautics,
Langley Field, Va., May 4, 1955.

REFERENCES

1. Whitcomb, Richard T.: A Study of the Zero-Lift Drag-Rise Characteristics of Wing-Body Combinations Near the Speed of Sound. NACA RM L52H08, 1952.

2. Carmel, Melvin M.: An Experimental Transonic Investigation of a 45° Swept Wing-Body Combination With Several Types of Body Indentation With Theoretical Comparisons Included. NACA RM L54I07a, 1954.

3. Holdaway, George H.: Comparison of Theoretical and Experimental Zero-Lift Drag-Rise Characteristics of Wing-Body-Tail Combinations Near the Speed of Sound. NACA RM A53H17, 1953.

4. Holdaway, George H.: An Experimental Investigation of Reduction in Transonic Drag Rise at Zero Lift by the Addition of Volume to the Fuselage of a Wing-Body-Tail Configuration and a Comparison With Theory. NACA RM A54F22, 1954.

5. Whitcomb, Richard T.: Recent Results Pertaining to the Application of the "Area Rule." NACA RM L53I15a, 1953.

6. Jones, Robert T.: Theory of Wing-Body Drag at Supersonic Speeds. NACA RM A53H18a, 1953.

7. Whitcomb, Richard T., and Fischetti, Thomas L.: Development of a Supersonic Area Rule and an Application to the Design of a Wing-Body Combination Having High Lift-to-Drag Ratios. NACA RM L53H31a, 1953.

8. Ward, Vernon G., Whitcomb, Charles F., and Pearson, Merwin D.: Air-Flow and Power Characteristics of the Langley 16-Foot Transonic Tunnel With Slotted Test Section. NACA RM L52E01, 1952.

9. Runckel, Jack F., and Schmeer, James W.: The Aerodynamic Characteristics at Transonic Speeds of a Model With a 45° Sweptback Wing, Including the Effect of Leading-Edge Slats and a Low Horizontal Tail. NACA RM L53J08, 1954.

10. Whitcomb, Charles F., and Osborne, Robert S.: An Experimental Investigation of Boundary Interference on Force and Moment Characteristics of Lifting Models in the Langley 16- and 8-Foot Transonic Tunnels. NACA RM L52I29, 1953.

11. Ritchie, Virgil S., and Pearson, Albin O.: Calibration of the Slotted Test Section of the Langley 8-Foot Transonic Tunnel and Preliminary Experimental Investigation of Boundary-Reflected Disturbances. NACA RM L51K14, 1952.

12. Blanchard, Willard S., Jr.: A Summary of the Low-Lift Drag and Longitudinal Trim Characteristics of Two Versions of an Interceptor-Type Airplane as Determined From Flight Tests of Rocket-Powered Models at Mach Numbers Between 0.75 and 1.78. NACA RM L54H31, 1954.

13. Bingham, Gene J., and Braslow, Albert L.: Subsonic Investigation of Effects of Body Indentation on Zero-Lift Drag Characteristics of a 45° Sweptback Wing-Body Combination With Natural and Fixed Boundary-Layer Transition Through a Range of Reynolds Number From 1×10^6 to 8×10^6. NACA RM L54B18a, 1954.

14. Carmel, Melvin M.: Transonic Wind-Tunnel Investigation of the Effects of Aspect Ratio, Spanwise Variations in Section Thickness Ratio, and a Body Indentation on the Aerodynamic Characteristics of a 45° Sweptback Wing-Body Combination. NACA RM L52L26b, 1953.

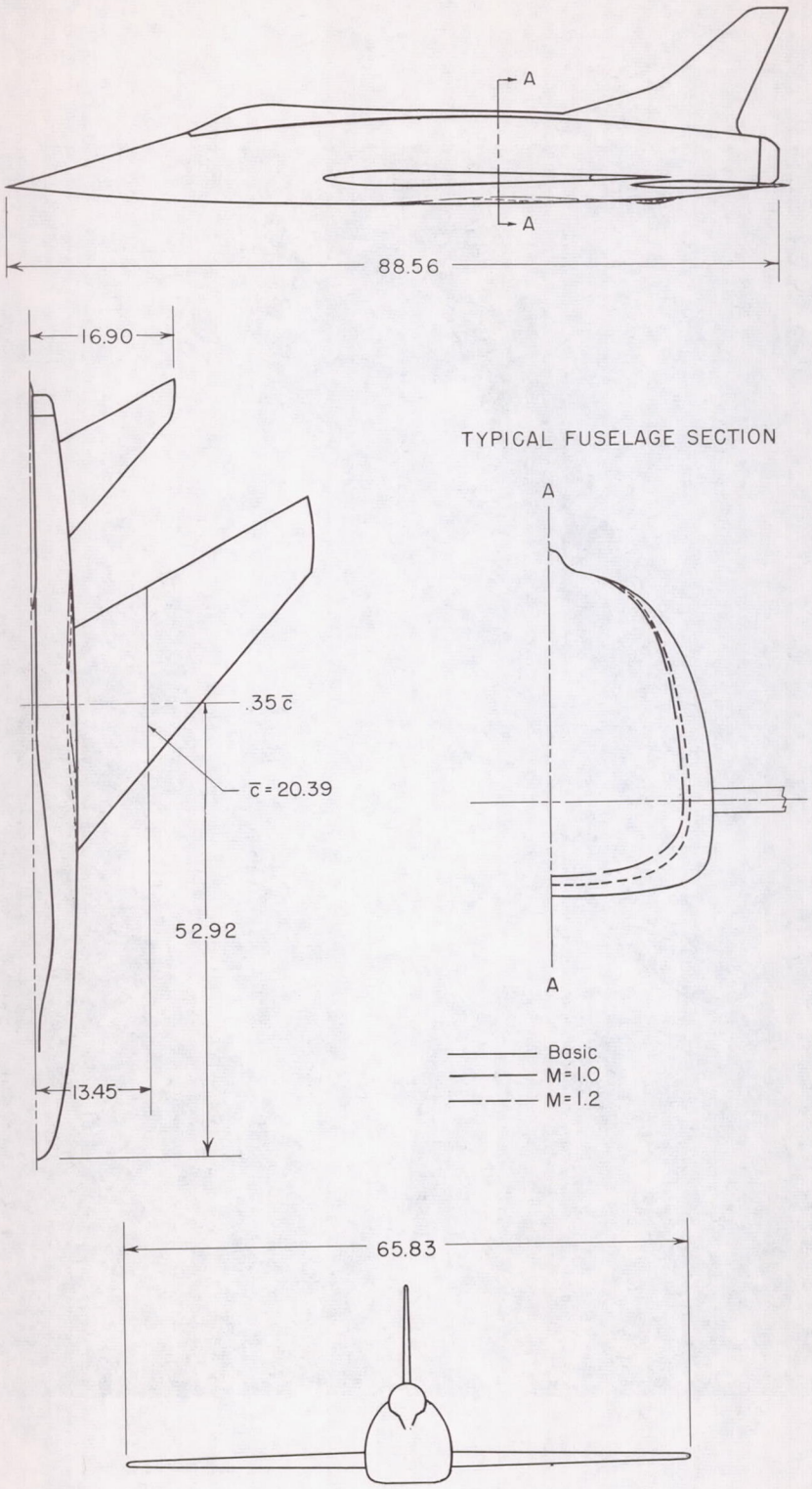

Figure 1.- Three-view drawing of the complete configurations. All dimensions are in inches.

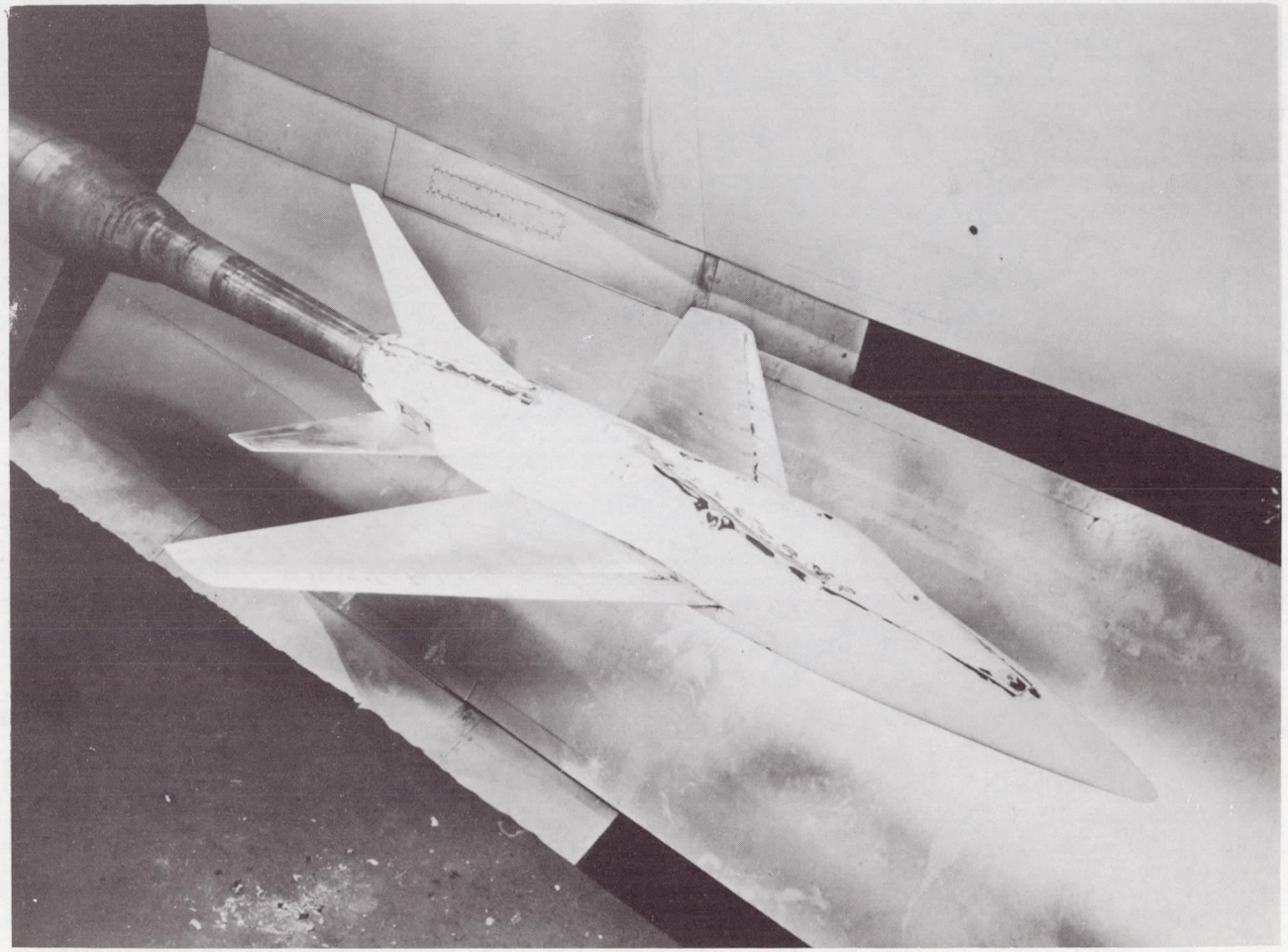

L-82817

(a) Complete basic configuration.

Figure 2.- Photographs of the models.

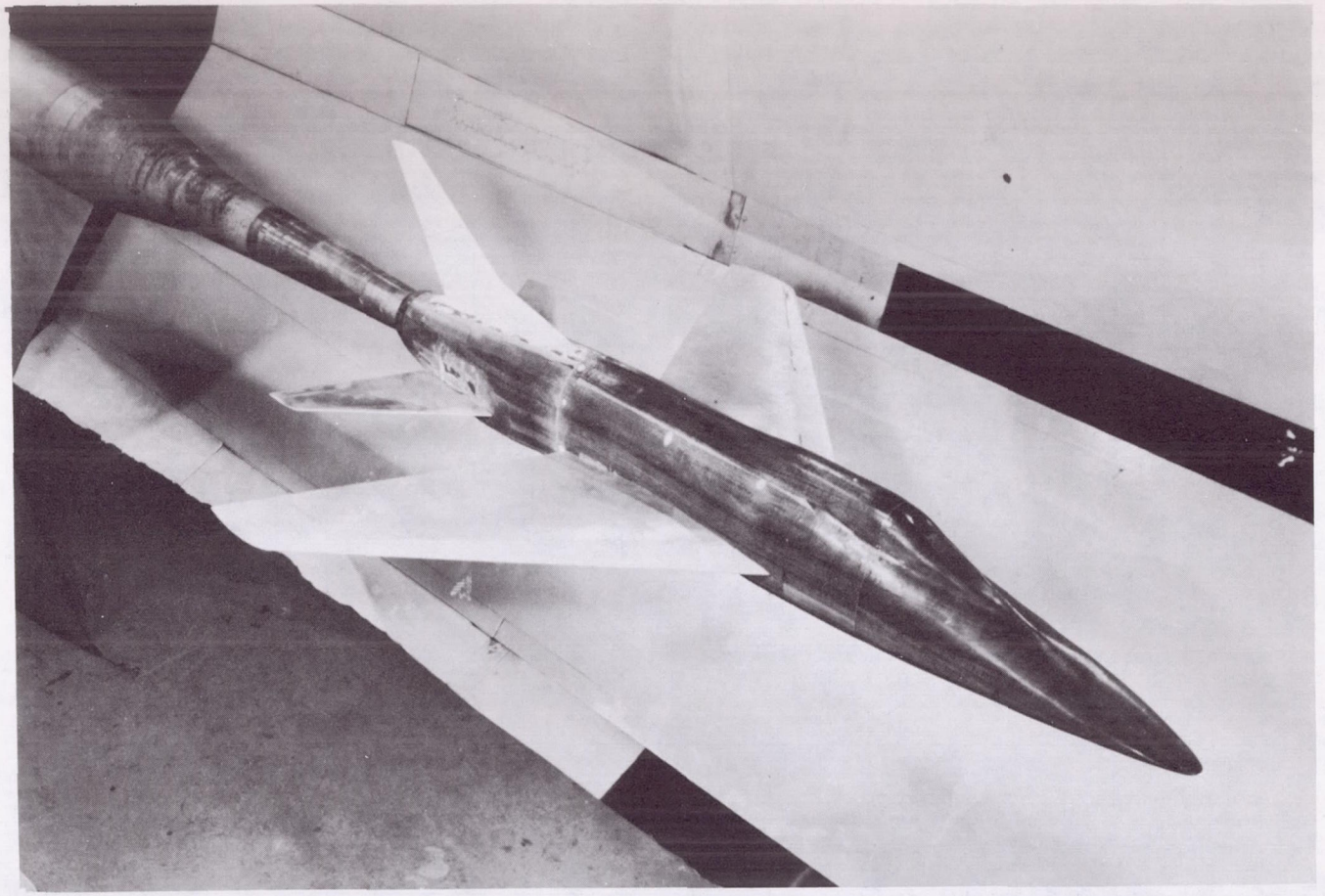

L-82818

(b) Complete M = 1.0 configuration.

Figure 2.- Concluded.

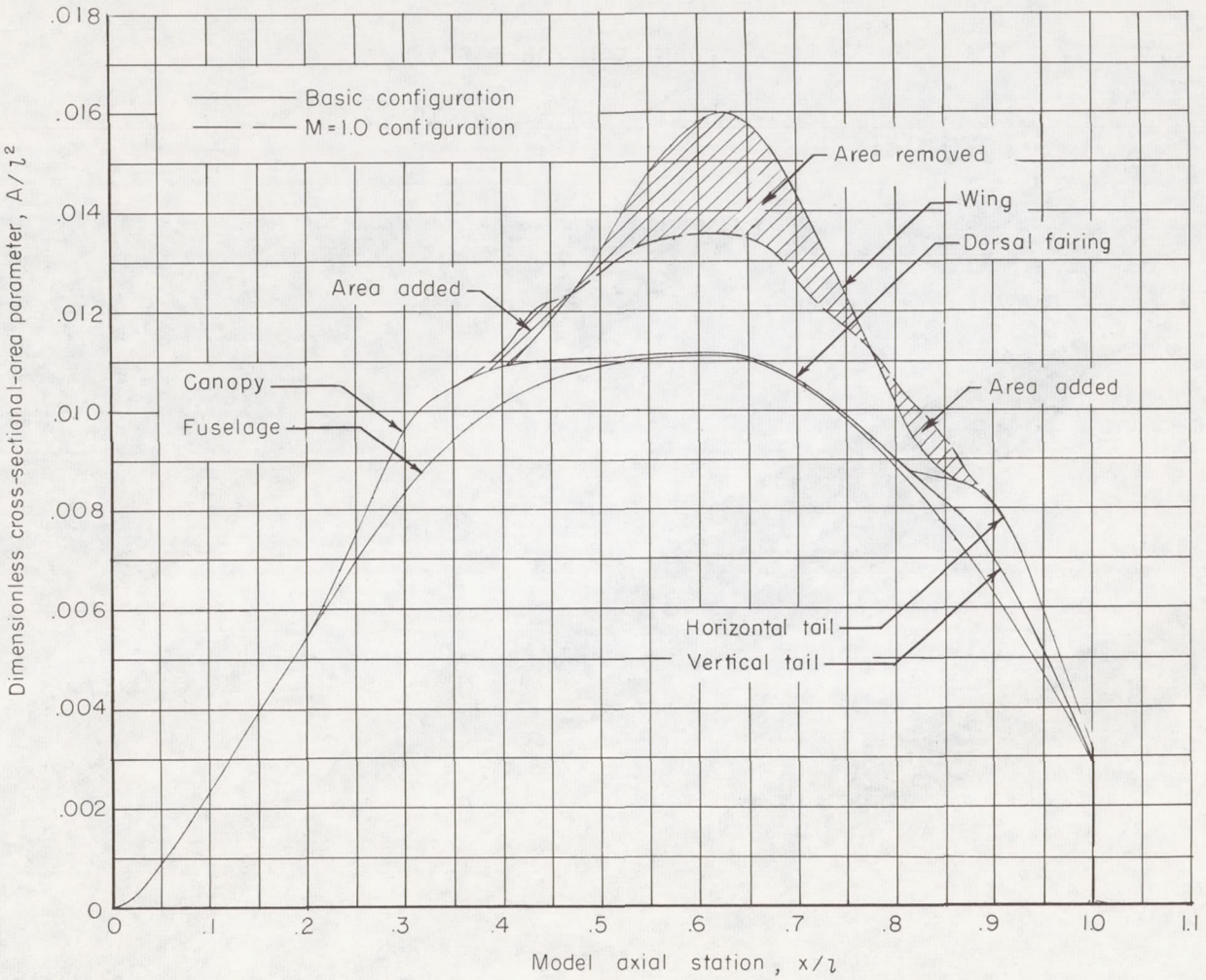

(a) Basic and M = 1.0 configurations.

Figure 3.- Model cross-sectional-area distributions.

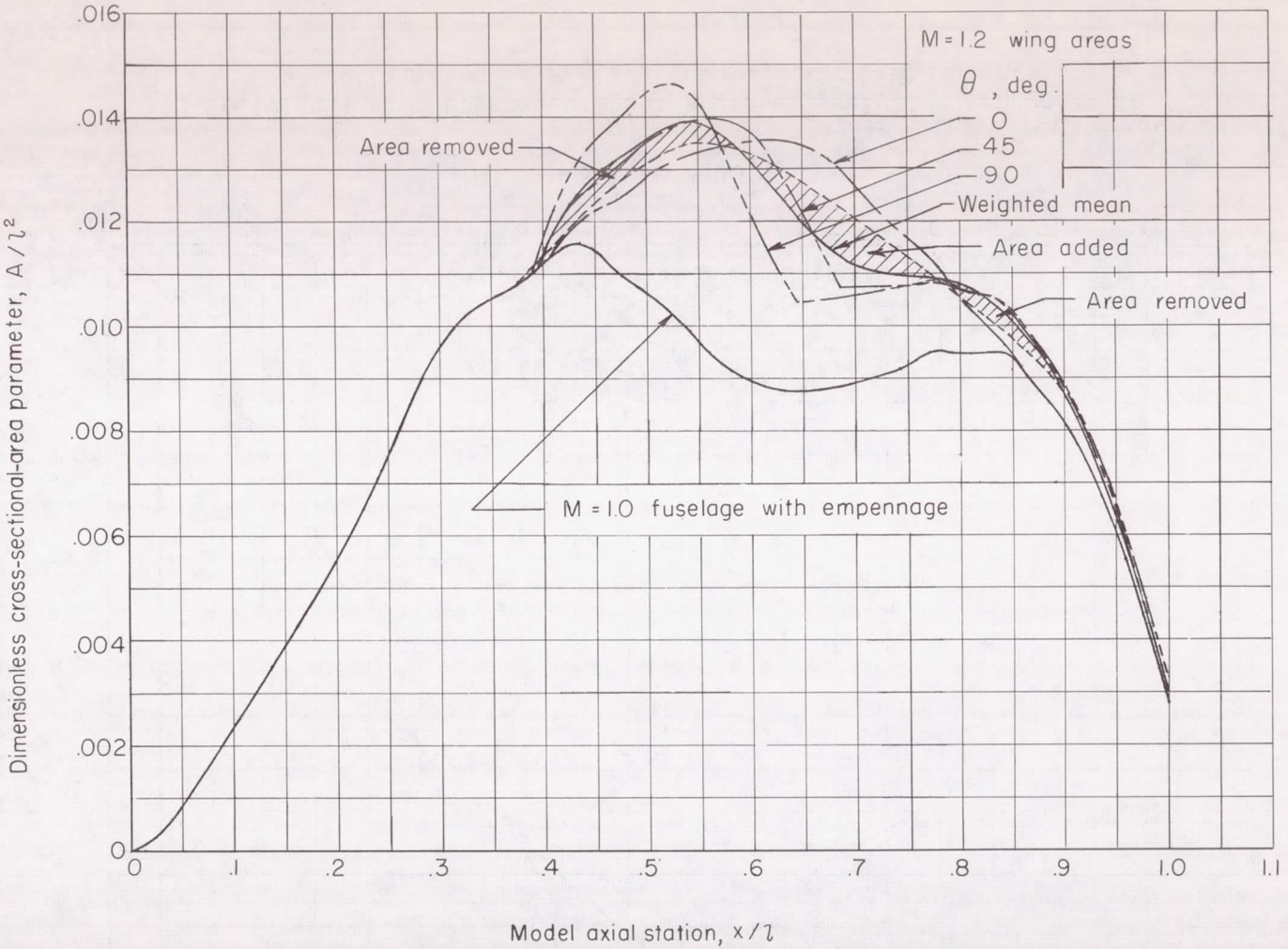

(b) Individual wing cross-sectional areas and weighted mean area at M = 1.2 imposed on M = 1.0 fuselage with empennage.

Figure 3.- Continued.

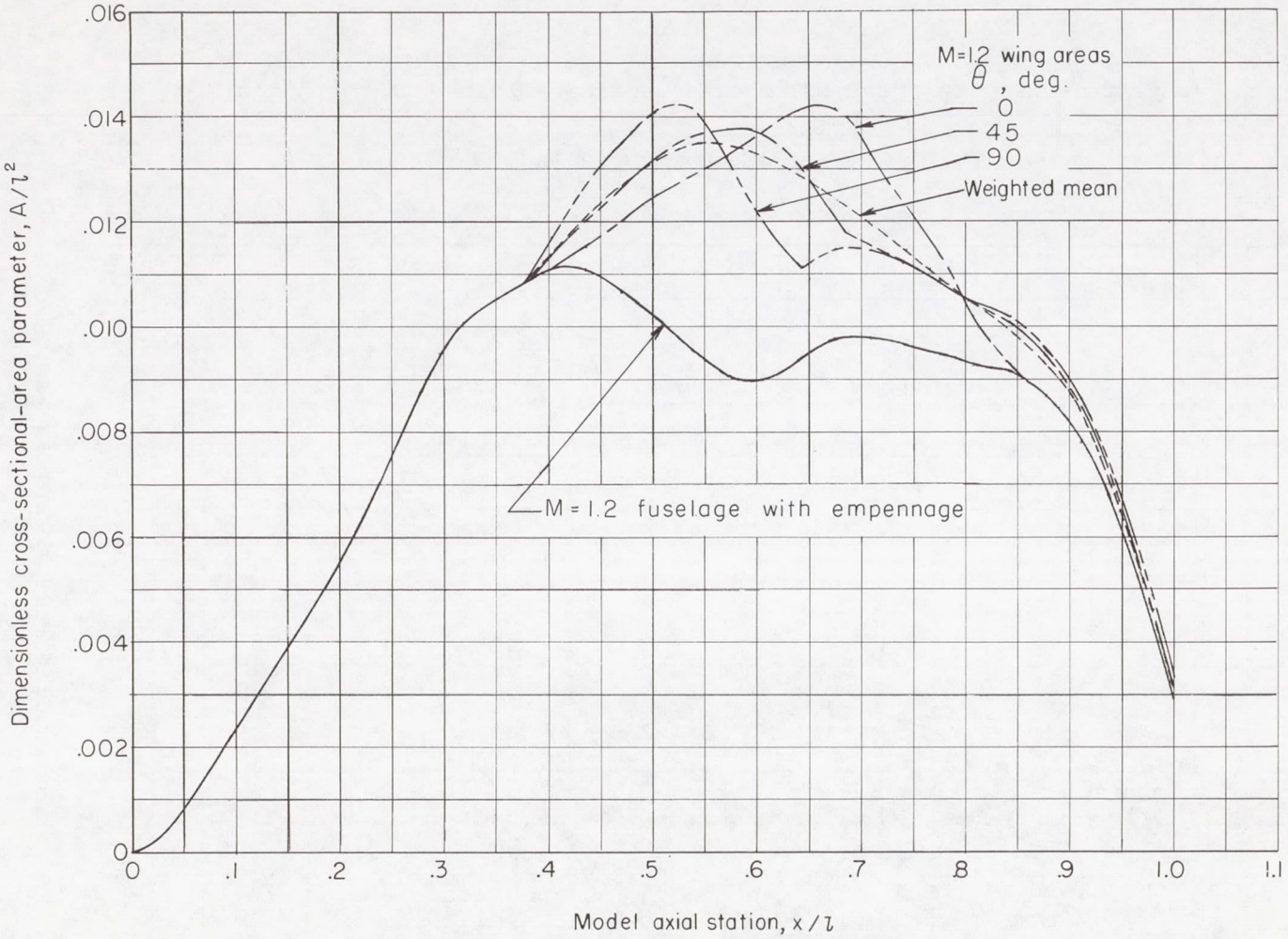

(c) Individual wing cross-sectional areas and weighted mean area at M = 1.2 imposed on M = 1.2 fuselage with empennage.

Figure 3.- Continued.

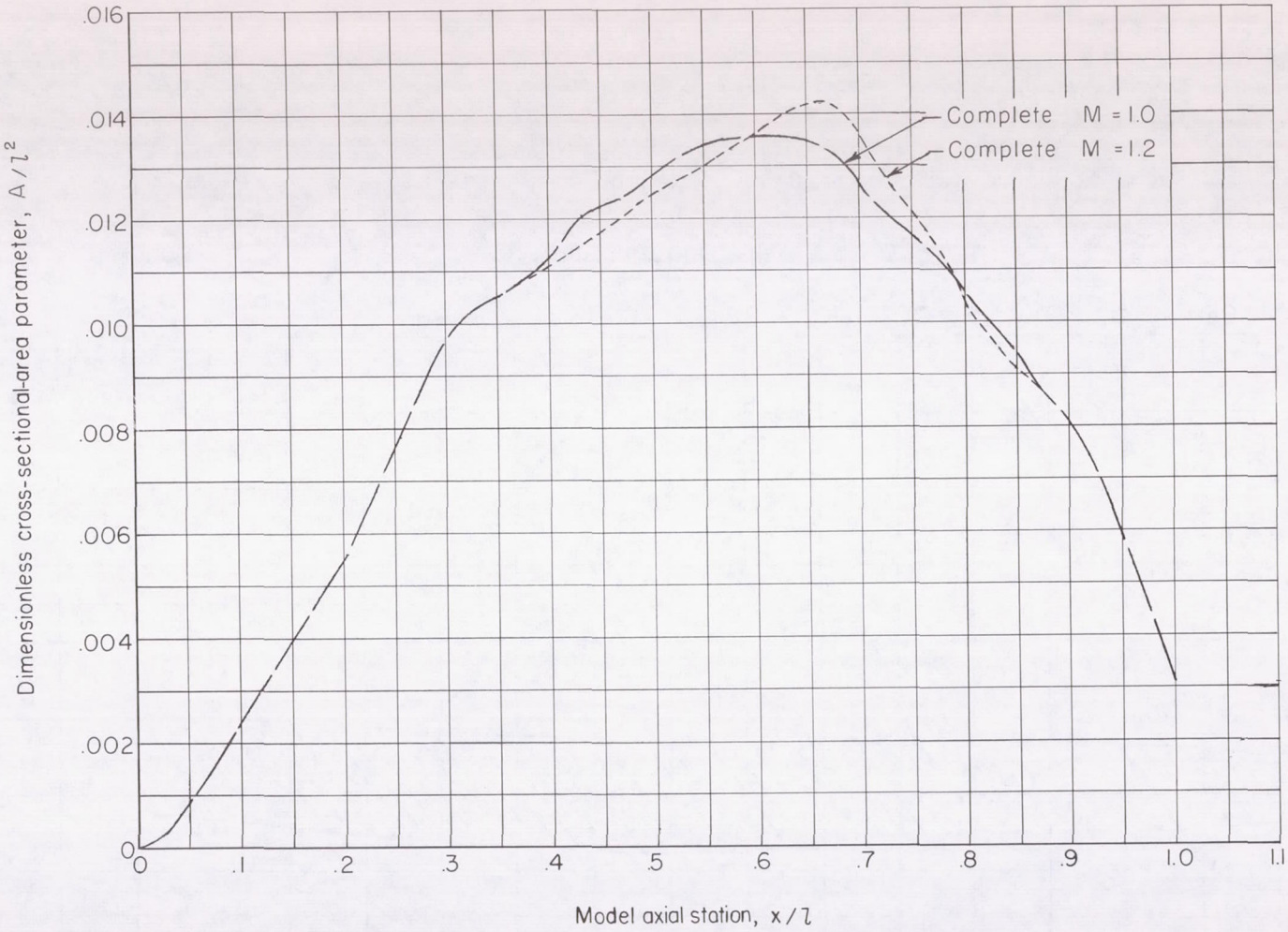

(d) Complete M = 1.0 and complete M = 1.2 configurations at sonic velocity.

Figure 3.- Concluded.

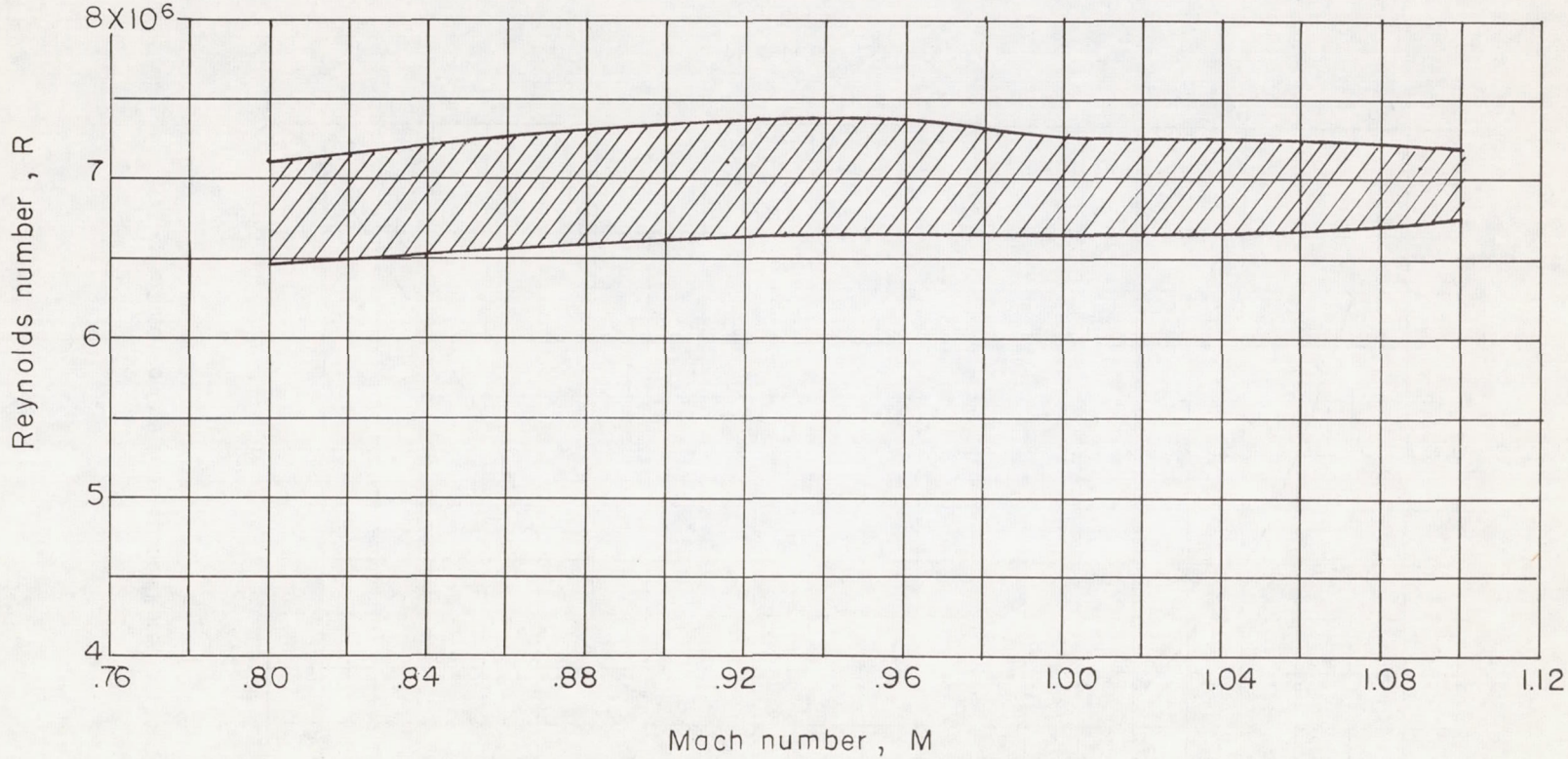

Figure 4.- Variation with Mach number of Reynolds number based on mean aerodynamic chord of 20.39 inches.

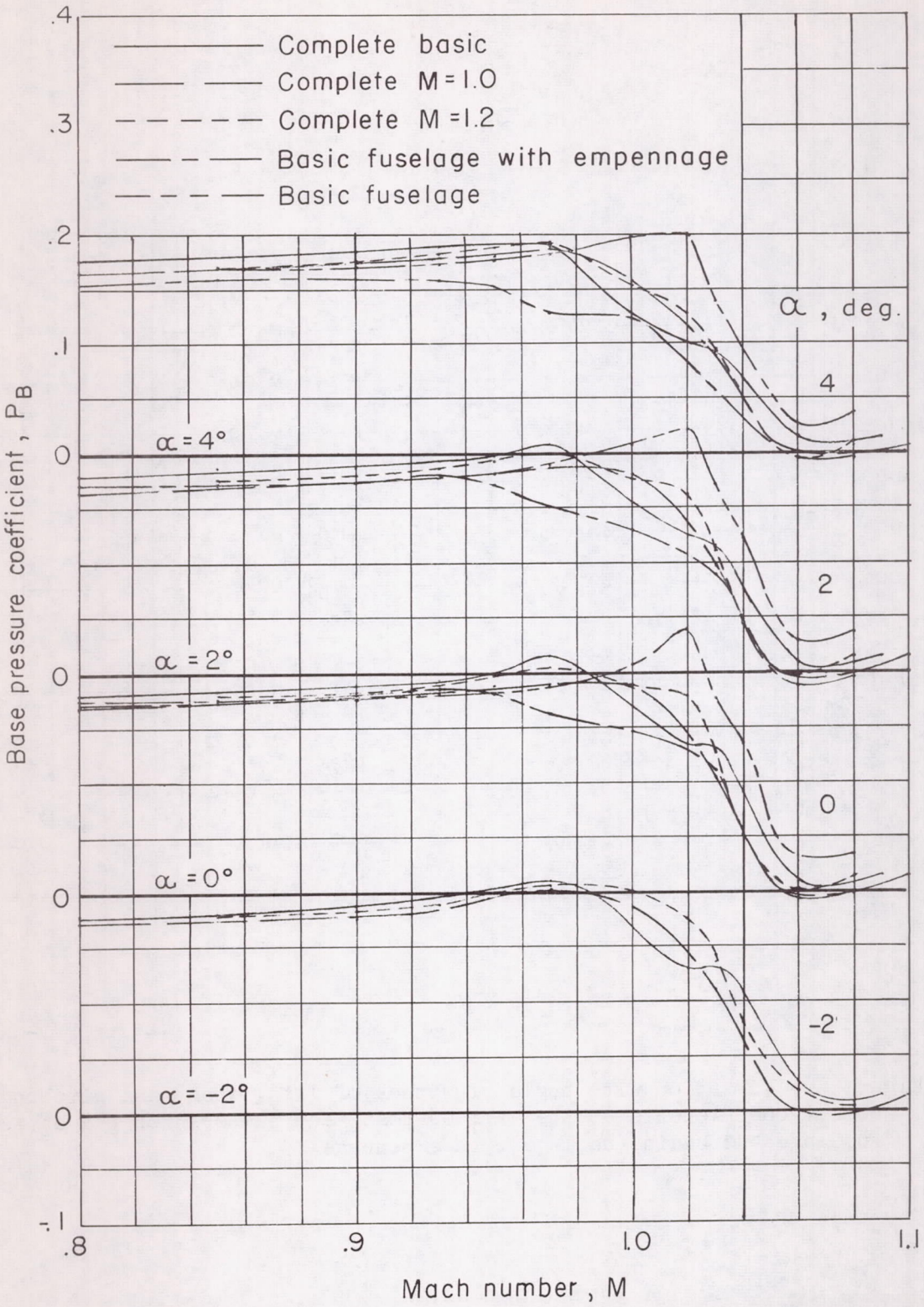

Figure 5.- Variation with Mach number of base pressure coefficient for the various configurations tested.

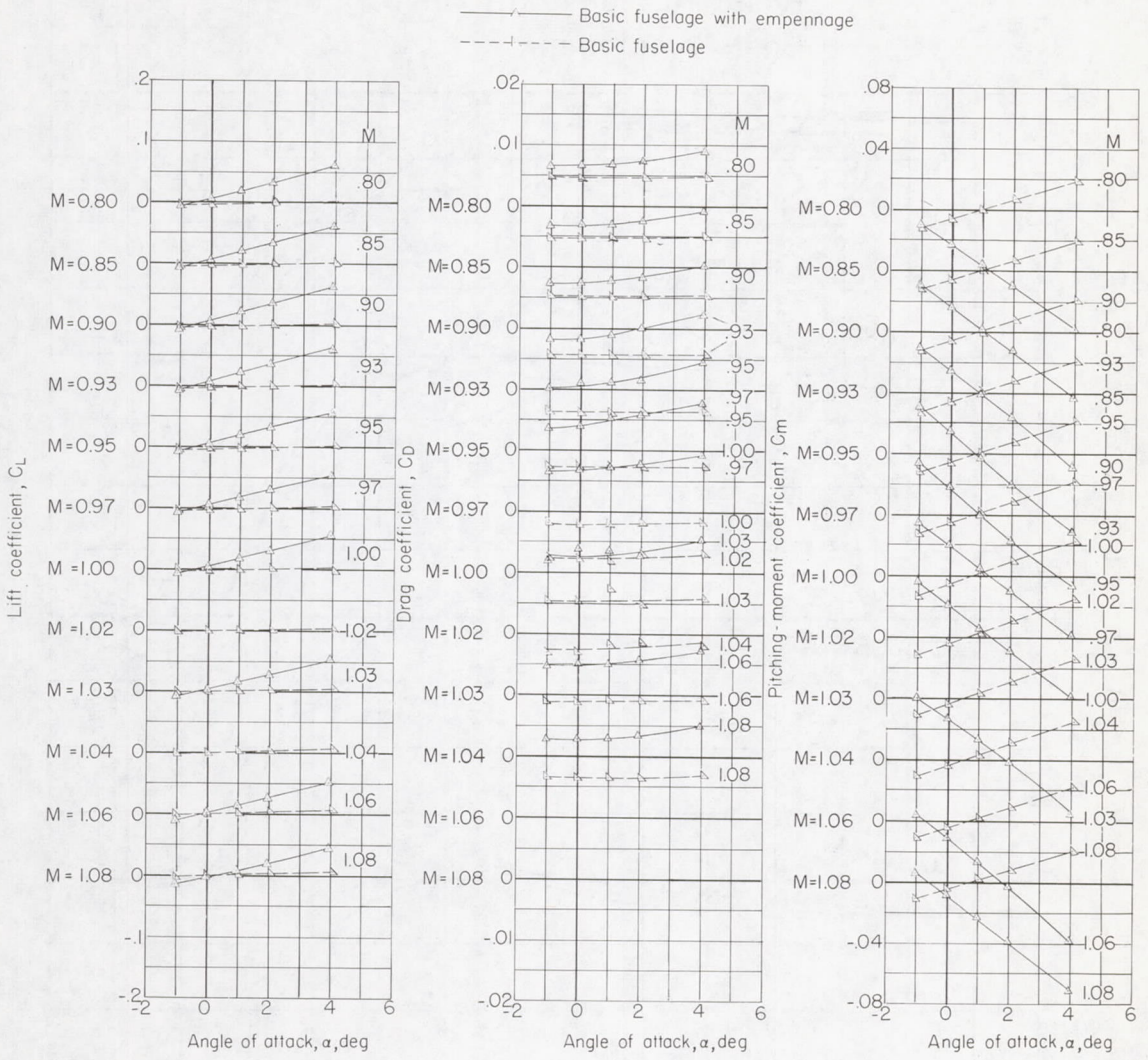

Figure 6.- Variation with angle of attack of lift, drag, and pitching-moment coefficients at the various test Mach numbers for the basic fuselage and basic fuselage with empennage.

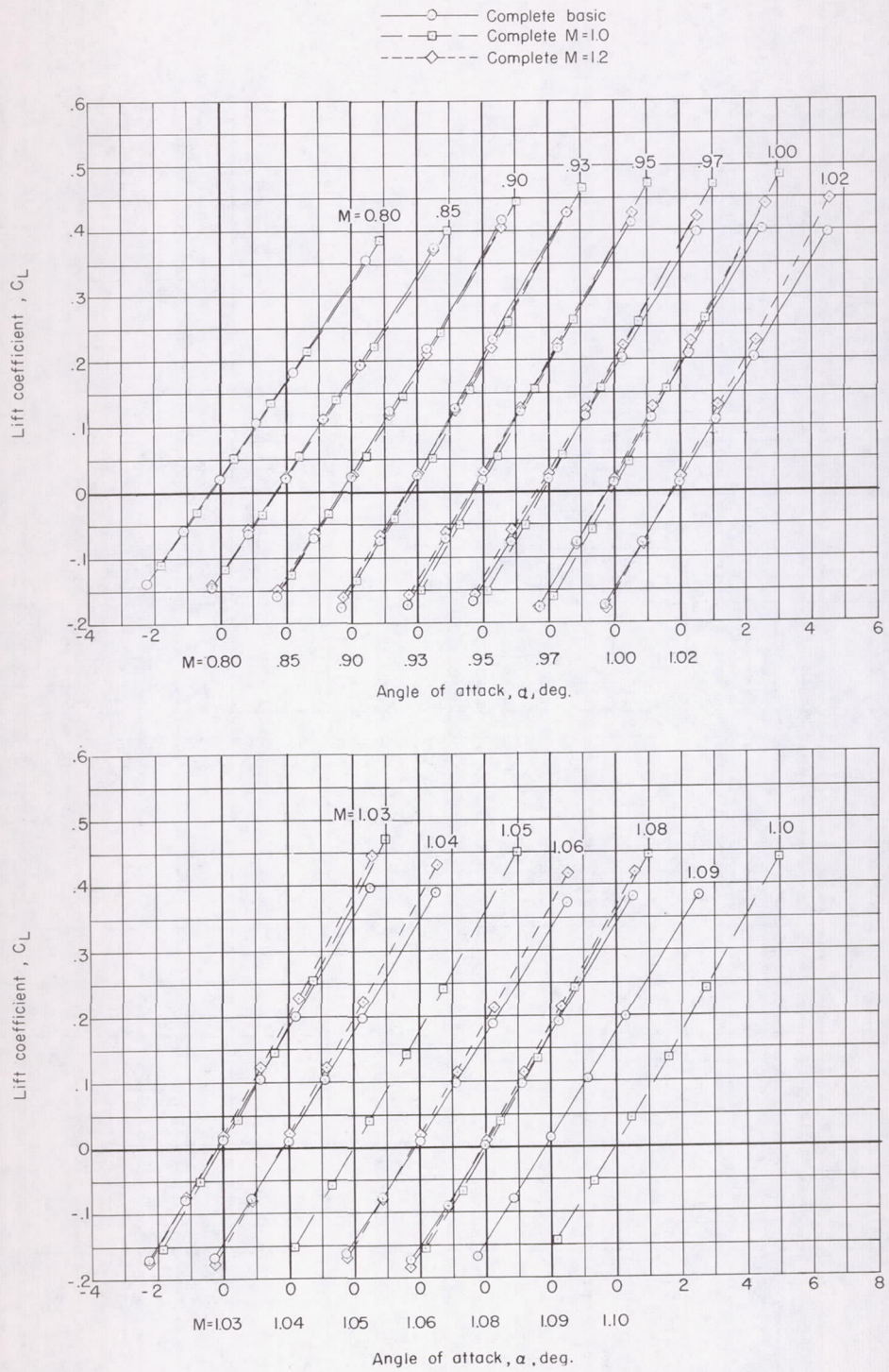

(a) Variation of C_L with α.

Figure 7.- Basic aerodynamic characteristics of the complete configurations.

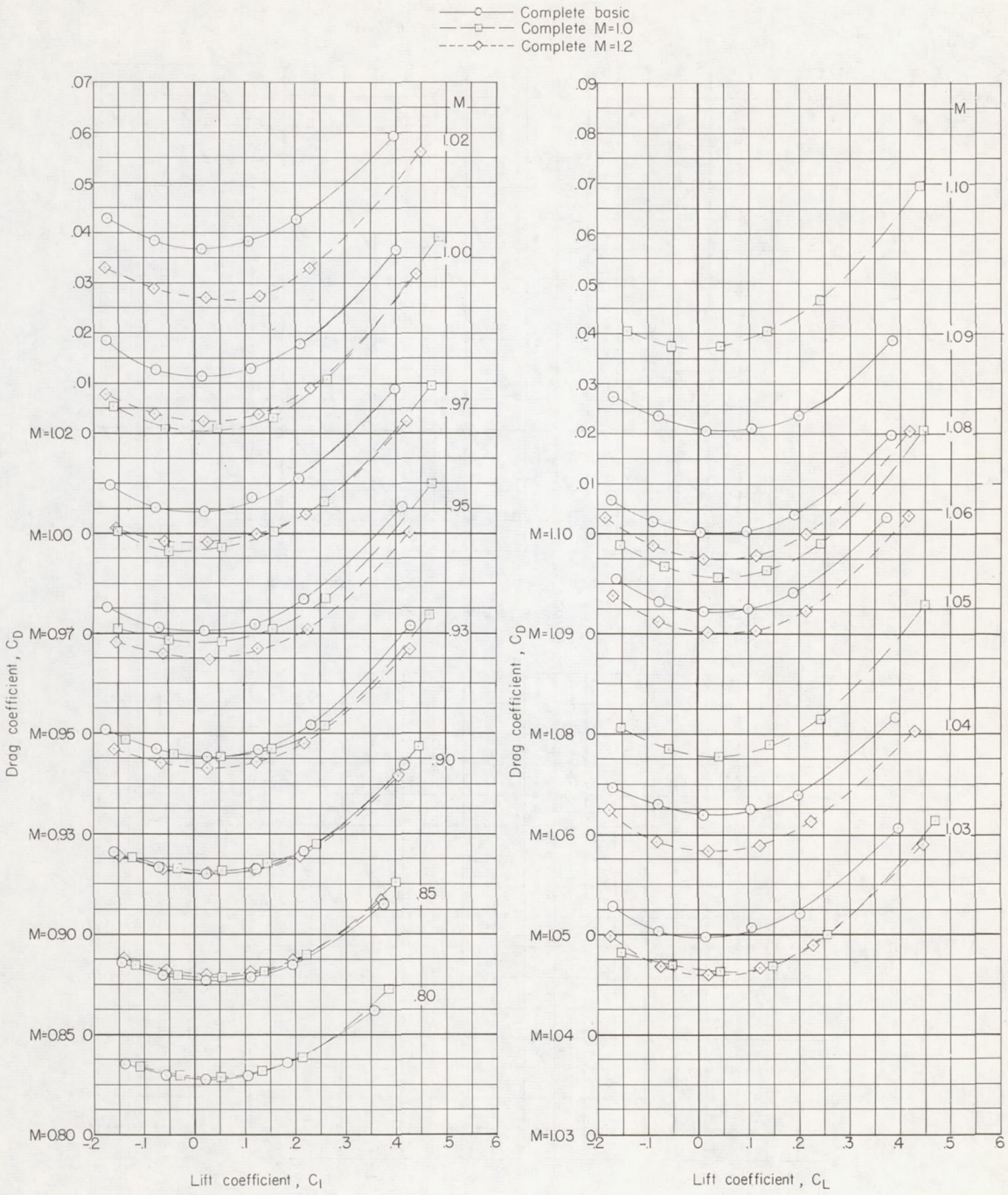

(b) Variation of C_D with C_L.

Figure 7.- Continued.

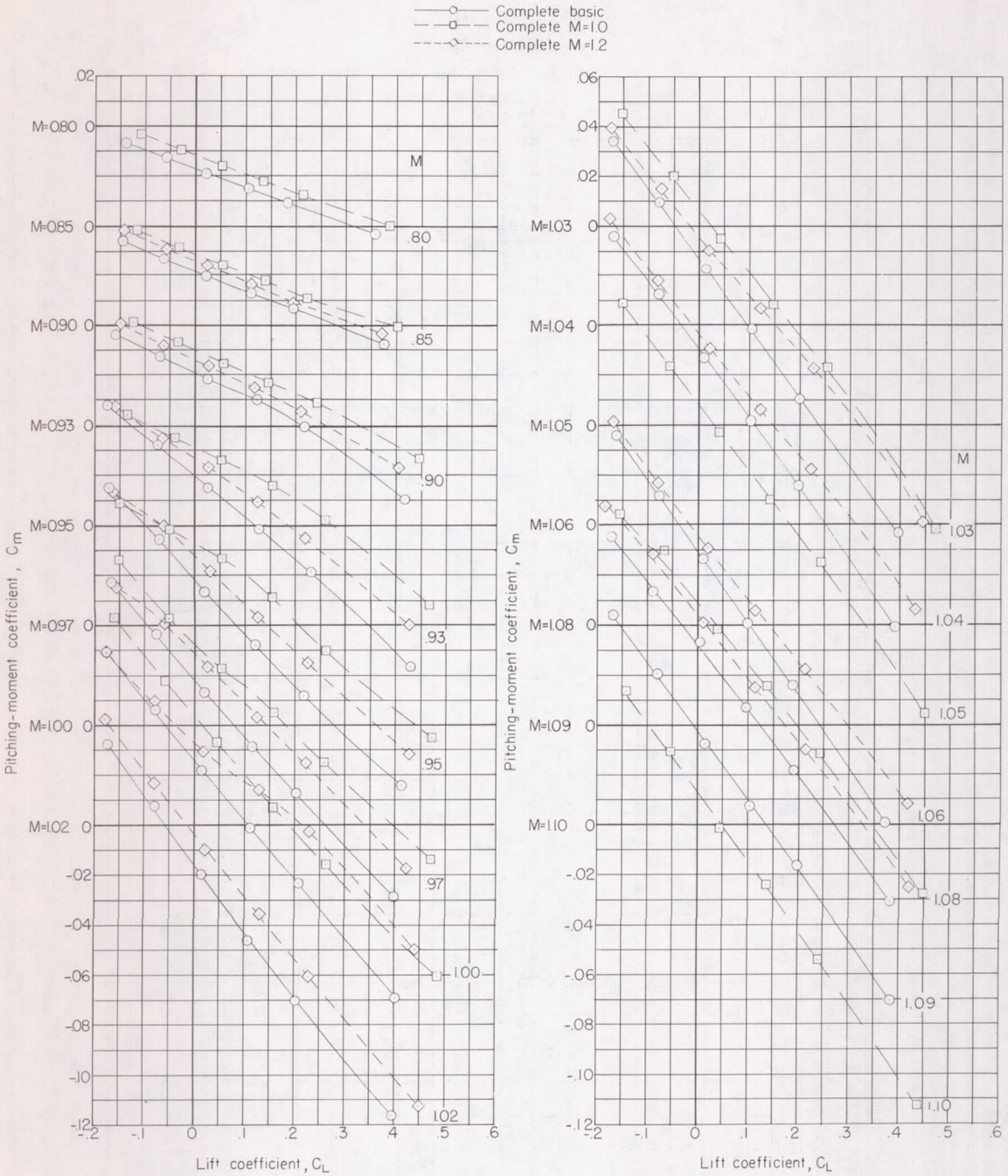

(c) Variation of C_m with C_L.

Figure 7.- Concluded.

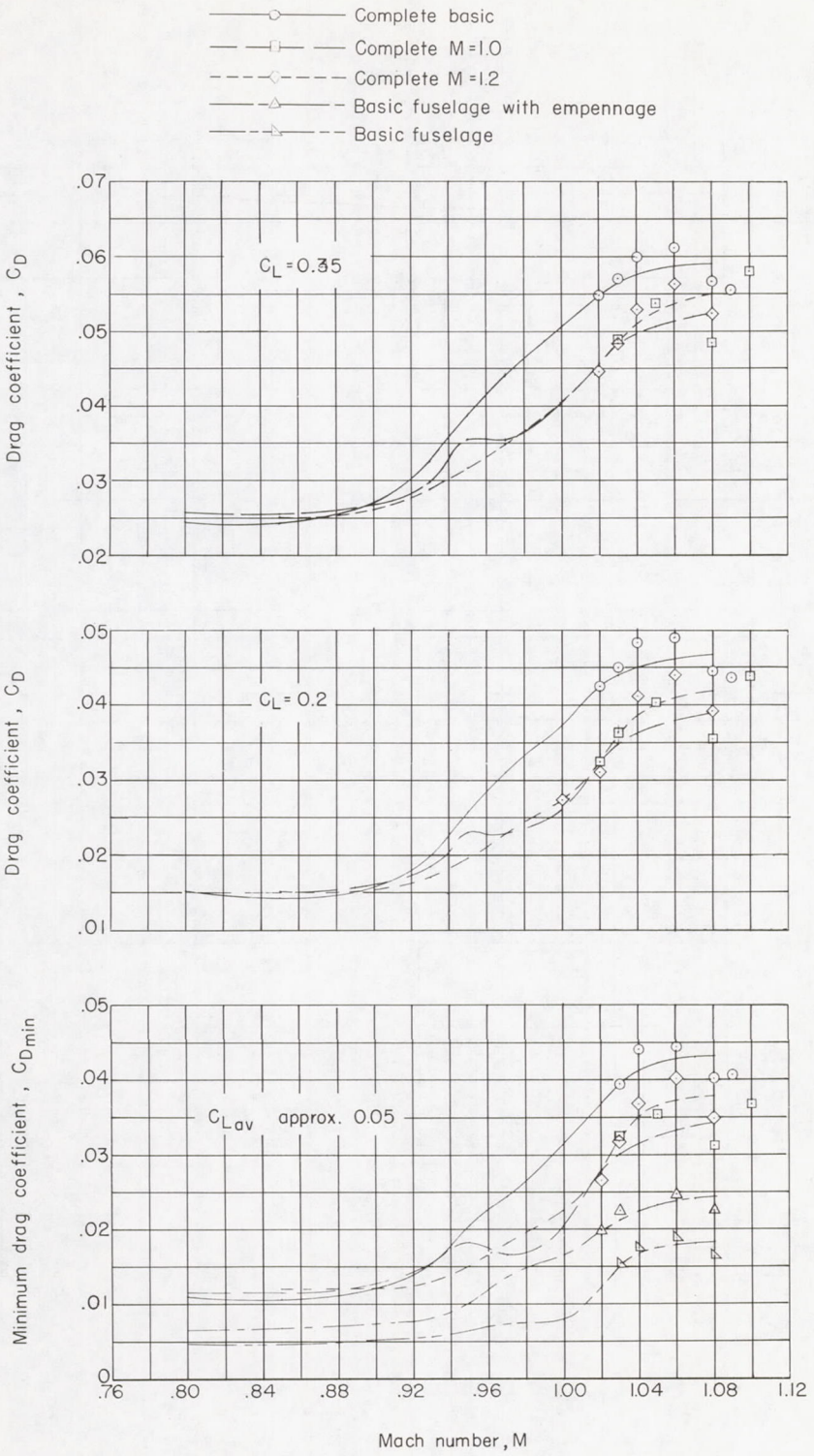

Figure 8.- Effect of Mach number on minimum drag coefficient and on drag coefficients at C_L = 0.2 and 0.35. Symbols indicate basic data.

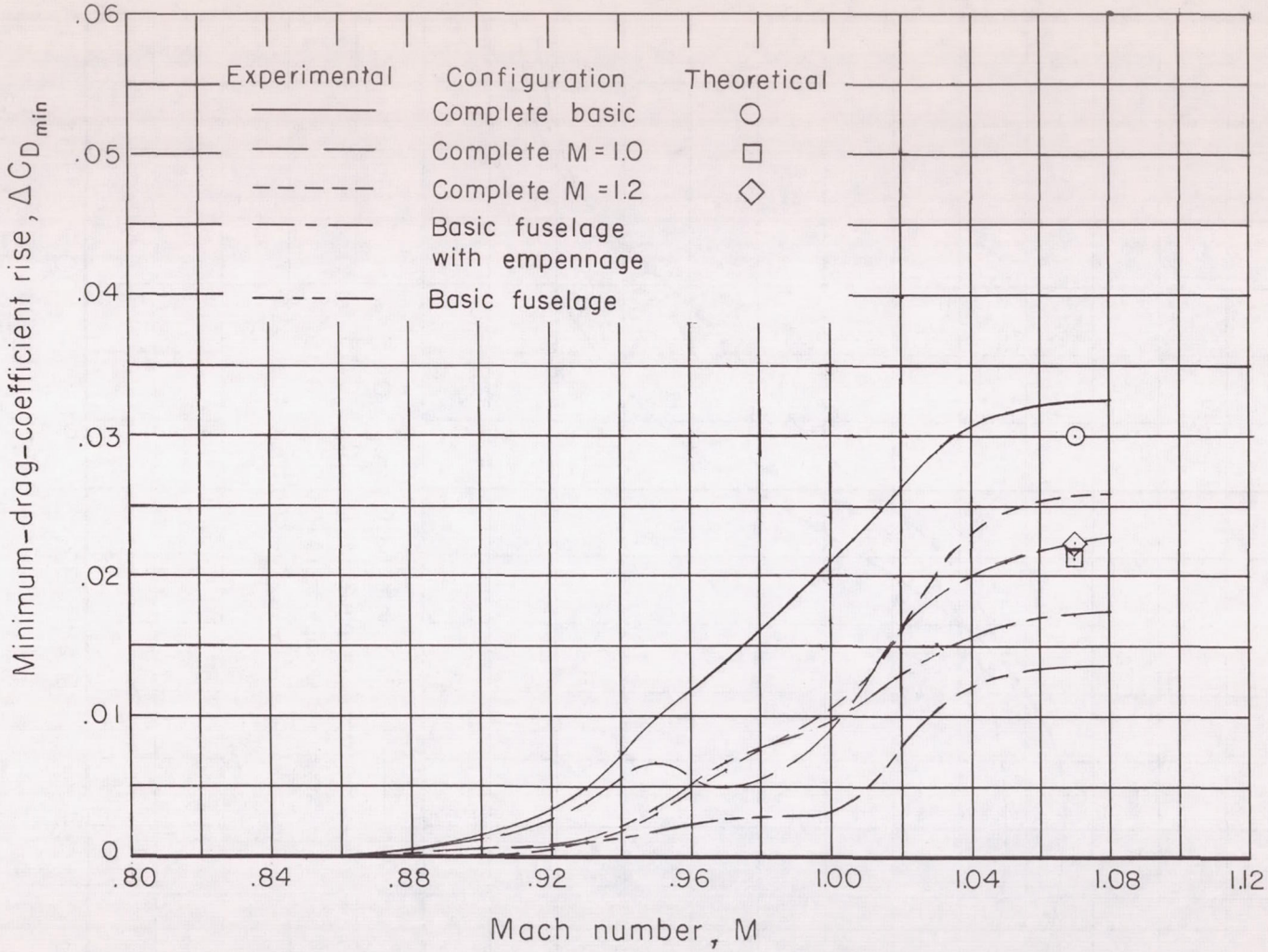

Figure 9.- Effect of Mach number on minimum-drag-coefficient rise. Symbols indicate values estimated theoretically by the method of reference 3.

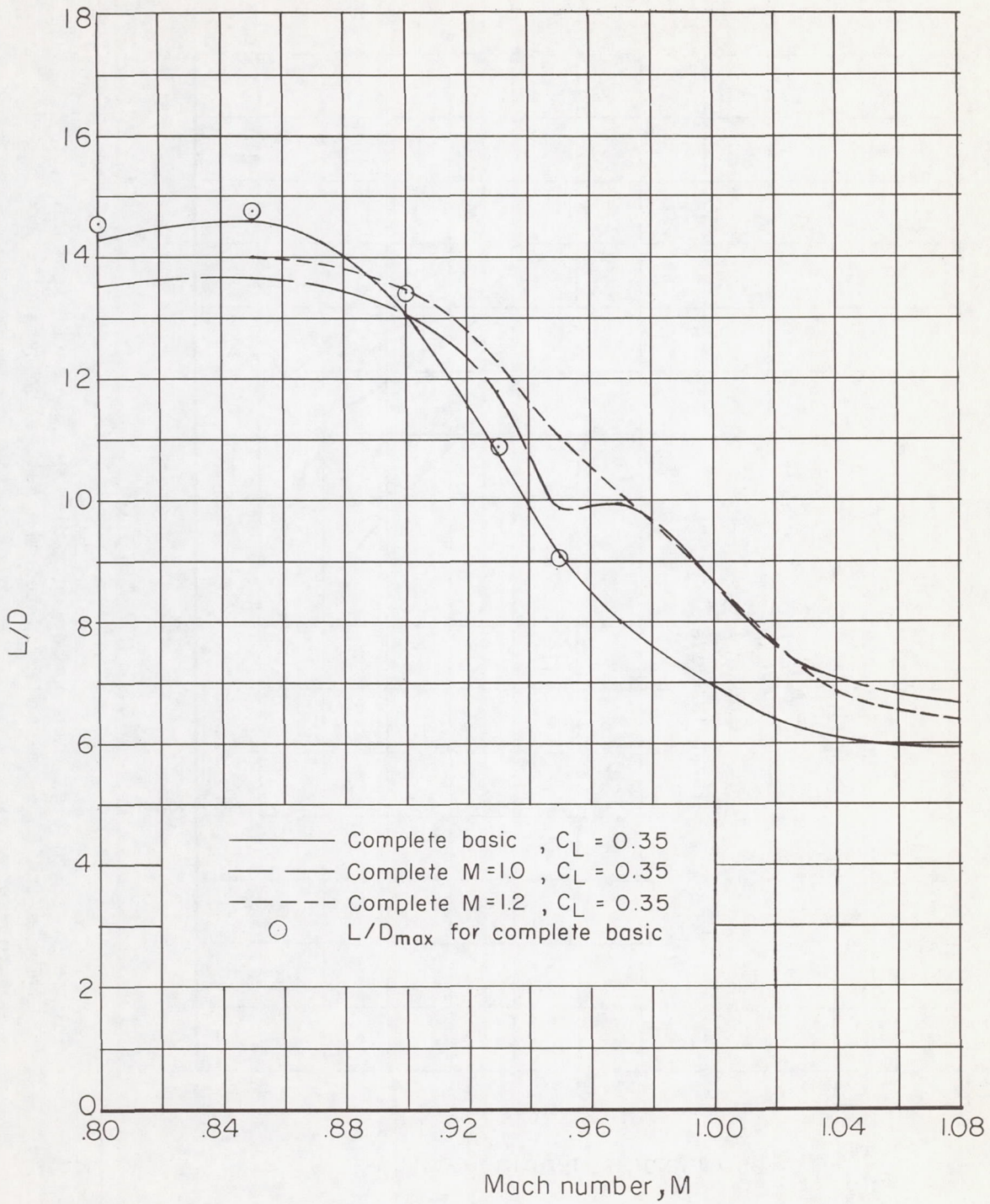

Figure 10.- Effect of Mach number on lift-drag ratios of the three complete configurations.